

Epitaxial Growth of Functional Oxides

Proceedings of the International Symposium

Editors

A. Goyal
Oak Ridge National Laboratory
Oak Ridge, TN, USA

Y. Kuo
Texas A&M University
College Station, TX, USA

O. Leonte
Berkeley Polymer Technology
Hayward, CA, USA

W. Wong-Ng
NIST
Gaithersburg, MD, USA



*Sponsoring Divisions:
Electronics, and Dielectric Science and Technology*

Proceedings Volume 2003-29



THE ELECTROCHEMICAL SOCIETY, INC.
65 South Main St., Pennington, NJ 08534-2839, USA

DEPOSITION of (211_{-1.0nm}/123_{-10nm})_xN MULTILAYER COATED CONDUCTORS on Ni-BASED TEXTURED SUBSTRATES

T. Haugan, P. Barnes, R. Nekkanti, J. M. Evans, L. Brunke, I. Maartense, J. P. Murphy
Air Force Research Laboratory, Propulsion Directorate, 2645 Fifth St. Bldg 450,
Wright-Patterson AFB, OH 45433-7919

A. Goyal, A. Gapud and L. Heatherly
Oak Ridge National Laboratory
1 Bethel Valley Road, Buildg. 4500S; Rm No. S-250
Oak Ridge, TN 37831-6116

ABSTRACT

Properties of multilayer (211_{-1.0nm}/123_{-10nm})_xN composite films deposited on buffer-coated rolling assisted biaxially textured (RABiT'sTM) Ni-alloy substrates were investigated providing initial results. Two different RABiT's substrates were tested: CeO₂/YSZ/CeO₂/Ni deposited in-situ prior to the YBCO composite deposition, and CeO₂/YSZ/Y₂O₃/Ni-3%W substrates prepared in an external process. Similar transport critical current densities (J_{cs}) at 77K in a self-field of ~ 0.6 -1.0 MA/cm² and transition temperatures (T_{cs}) ~ 89 -90 K were obtained for films deposited onto both architectures. These results were consistently achieved for the initial deposition parameters chosen on both substrates; no process optimization was conducted in this report. Compared to 123 films deposited on similar substrates, transport J_{cs} (77K, H_{appl}) were reduced slightly for $H_{appl} \sim < 1.5$ T, but increased on average for $H_{appl} > 1.5$ T. However, this is contrary to results on single crystals which had improved current densities even at $H_{appl} \sim < 1.5$ T; i.e. where some optimization has occurred. The surface microstructure of the multilayer films on RABiT's substrates showed flat surfaces and greatly reduced particulate formation, similar to multilayer deposition on single crystal substrates. However void formations were observed similar to deposition of 123 on RABiT's, which presumably predominately resulted from defects in the buffer layer structure.

INTRODUCTION

The development of coated conductor wires using YBa₂Cu₃O_{7- δ} (123) on buffer-coated Ni-alloy substrates with critical current density $J_c > 1$ MA/cm² offers great promise for incorporating YBCO coated conductors in applications such as transformers, generators, or motors operating at 77 K [1-7]. Critical current densities > 1 MA/cm² have been achieved on long length metallic substrates with the use of the rolling assisted biaxially textured (RABiT'sTM) process, which creates a high degree of a-b in-plane grain alignment in Ni-alloys and in subsequent epitaxial deposition of buffer layers and 123 film [7]. YBa₂Cu₃O_{7- δ} films have excellent properties at 77 K including high critical current densities (J_c) due to good flux pinning in applied magnetic fields, which is critical for most applications [1,2]. Typically for magnetic fields applied in the least favorable

orientation $H_{\text{appl}} // c\text{-axis}$, J_c will decrease by a factor of 10 to 100 with $H_{\text{appl}} = 1 \text{ T to } 5 \text{ T}$ [8,9]. It is of interest to increase J_c even further in applied fields, as such improvements can not only lower overall system costs for applications, but also allow for reductions in the weight and size of the system.

This paper considers the deposition of composite films with the architecture $(211_{-1.0\text{nm}}/123_{-10\text{nm}}) \times N$ on RABiT's substrates to improve the flux pinning. Deposition of multilayer $(211_{-1.5\text{nm}}/123_{-10\text{nm}}) \times N$ composite films on LaAlO_3 single crystal substrates was recently demonstrated to provide significant improvement of $J_c(H)$ up to $\sim 300\%$ in applied fields of ~ 0.1 to $\sim 1.6 \text{ T}$ [10]. In the multilayer composite structure, $\sim (10\text{-}15 \text{ nm size } \text{Y}_2\text{BaCuO}_5 (211) \text{ nanoparticles are deposited by the island-growth method resulting in a 211 particulate dispersion as opposed to a uniform layer. This layer of dispersive nanoparticles is separated by 123 film layers of thicknesses typically } \sim (5\text{-}15) \text{ nm. The area number density of 211 nanoparticles is on the order of } (1.5\text{-}3) \times 10^{11} \text{ cm}^{-2}$ which is sufficient to provide a pinning density equivalent to a (3-6) T applied magnetic field fluxon density. This multilayer structure has been repeated with up to 200 bilayers thus far, with the layered structure and surface flatness maintained. Other advantages of the multilayer films include reduced particulate defect formation, and possibly improved mechanical crack resistance as a consequence of integration of the high density of nanoparticles into the film structure [10]. The decreased surface roughness of the layers is believed to be related to renucleation and minimizing of the 123 grain size.

While these properties and advantages are useful, it is necessary to further demonstrate that such properties can be achieved on textured buffered substrates. A significant difference between RABiT's substrates and single crystal substrates is the presence in RABiT's substrates of $(0\text{-}8)^\circ$ grain boundaries, which reduces J_c on average [2]. The possible effect of 211 nanoparticle depositions at these grain boundaries is preliminarily discussed. The main emphasis of this paper is to present initial investigations of multilayer $(211_{-1.0\text{nm}}/123_{-10\text{nm}}) \times N$ film deposition on Ni-alloy RABiT's substrates.

EXPERIMENTAL

Multiple layers of 123 films and 211 nanoparticles were deposited by pulsed laser deposition, using parameters and conditions described in detail previously [10,11]. The laser ablation targets were purchased commercially (Superconductive Components Inc., Columbus OH). The 123 target was 92 % dense and made using powder processed by chemical precipitation (nominally 99.999 % pure), and the 211 target was 87-88 % dense made with solid-state powders (99.9 % purity). The depositions were automated and controlled, with the laser pulses trigger-actuated by computer control. Film growth was stopped between each layer for a period of about 13 seconds, when the other target was rotated into position. An excimer laser (Lambda Physik, model LPX 305i) operating at 248 nm was used. The laser fluence was $\sim 3.2 \text{ J/cm}^2$ and the ablation spot size was $\sim 1 \times 6.5 \text{ mm}^2$. The laser pulse rate was 4 Hz. The target-to-substrate distance was 6 cm. The oxygen deposition pressure was 300 mtorr for both 211 and 123 phases, as measured with capacitance manometer and convectron gauges within $< 10\%$ variation. Oxygen gas (99.999% purity) flowed into the chamber during growth at $\sim 1 \text{ l/min}$, and the oxygen pressure in the chamber was kept constant in the chamber using a downstream throttle-valve control on the pumping line. The laser beam was scanned across (1.6-2.0) cm of the 2.5 cm diameter targets to improve the film thickness uniformity in the deposition zone. The LaAlO_3 (100) and SrTiO_3 (100) single crystal substrates were ultrasonically

cleaned for 2 minutes each using first acetone, followed by dehydrated ethyl alcohol or isopropyl alcohol. Crystal substrates were provided by the manufacturer epitaxially polished on both sides for LaAlO_3 and on one side for SrTiO_3 , and were attached to the heater using a thin layer of colloidal Ag paint. Substrates sizes were $3.2 \times 3.2 \text{ mm}^2$ for magnetic J_c measurements, $3 \times 12 \text{ mm}^2$ single crystals and $\sim 4.5 \times 25 \text{ mm}^2$ RABiT's substrates for transport J_c measurements.

The background pressure in the chamber was reduced to $< 10^{-6}$ Torr prior to depositions. Samples were heated from room temperature to deposition temperature of 785°C at 1270°C/h . After deposition, films were cooled from 785°C to 750°C at 1270°C/h before turning off the vacuum pumps and O_2 pressure control. Subsequently the O_2 flow was increased to $\sim 1.5 \text{ l/min}$ into the chamber. The films were then cooled from 750°C to 500°C at a rate of 1270°C/h , and held at 500°C for 30 minutes, during which the O_2 pressure reached 1 atm. The films were cooled from 500°C to 250°C at about 1250°C/h , and from 250°C to room temperature using the natural cooling rate of the heater block ($\sim 800^\circ\text{C/h}$).

The 123 layer and 211 "pseudo" layer thickness was closely estimated by calibrating the deposition rates of both 123 and 211 for many deposition runs both before and after multilayer depositions. Although the 211 layer contains discontinuous nanoparticles, a 211 'pseudo' layer thickness was calculated assuming a smooth continuous layer. For similar conditions, 211 was observed to deposit on Zr(Y)O_2 or LaAlO_3 substrates at a slightly higher rate, with the ratio of deposition rates for (211/123) being 1.26 ± 0.09 . After measuring the total film thickness of the composite structure film, this ratio together with the number of pulses was used to determine the relative 123 and 211 pseudo layer thickness achieved for each composite film.

Buffer layers were applied in-situ at AFRL on as-rolled Ni tape using the following process. After a holding period of 10 min at a heater block temperature of 750°C , a CeO_2 seed layer was deposited in a forming gas (95%Ar,5% H_2) for 2 min at a 4 Hz laser repetition rate. A vacuum was then created in the chamber and the deposition of CeO_2 was continued for an additional 1.0 min. Oxygen gas was then introduced into the chamber and after stabilizing the pressure at $\sim 10^{-4}$ torr, the CeO_2 layer was further deposited for 1.2 min. The temperature was then increased to 780°C , and the YSZ buffer layer was deposited for 20 min in the same oxygen atmosphere using a 10 Hz frequency. A cap layer of CeO_2 was then deposited at a 4 Hz repetition rate for 1.5 min. Laser fluence for all buffer layers deposited was $\sim 3.2 \text{ J/cm}^2$. The oxygen pressure was subsequently increased to 300 mtorr and the multilayers were deposited as described above.

Buffered Ni-3%W substrates from ORNL were prepared as following. The as-received rolled Ni-3%W tape was annealed at 1250°C for 20 minutes in a vacuum chamber containing 3×10^{-7} Torr of H_2S . This produced a sulfur superstructure on the surface of the alloy. After annealing, the tape was rewound to its starting position, and a seed layer of Y_2O_3 was deposited in the same chamber using a reactive electron beam evaporation method. Yttrium metal was evaporated in the presence of 5×10^{-5} Torr H_2O . The tape was then transferred to another chamber and the YSZ and CeO_2 layers were deposited using a RF magnetron sputtering process. YSZ and CeO_2 targets were sputtered in the presence of 3 and 8×10^{-5} Torr H_2O , respectively. The thickness of the buffer layers were Y_2O_3 - 30nm, YSZ - 200nm, and CeO_2 - 25nm. Reference films of 123 on Ni RABiT's substrates of similar thickness as multilayer tapes about $0.34 \mu\text{m}$ were made and measured at ORNL by the BaF_2 process [12].

After deposition, current and voltage contacts for J_c measurements were patterned onto the films by DC magnetron sputter deposition of Ag with $\sim 3 \mu\text{m}$ thickness. The resistance of the Ag-123 contacts was reduced by annealing in pure O_2 at 550°C for 30 minutes, followed by annealing at 500°C for (0.5-2) hrs, with heating and cooling rates of 200°C/h [13]. Critical currents were measured over macrobridges 0.3 cm long and 0.05 cm wide, patterned using 248 nm KrF laser etching through a precisely machined Al_2O_3 mask or using standard chemical resist lithographic methods. The film thickness of every sample on LaAlO_3 substrates was measured multiple times across acid-etched steps next to or directly across bridges with a P-15 Tencor profilometer, and with SEM cross-sections. Care was used to measure with the profilometer only in twin-free areas of the LaAlO_3 substrates, which were observed visually at high magnification. For RABiT's substrates, the thickness variation for depositions was measured from run-to-run, and an average thickness from these runs was used to estimate the final thickness of the YBCO on the RABiT's substrates.

For transport J_c measurements at Oak Ridge National Laboratory (ORNL), the temperature for measurement was stable within $\pm 0.008 \text{ K}$. The whole width of the tape was used for J_c with an estimated width of 4.5 mm for computation of J_c ; the irreversibility (H_{irr}) criterion was determined using the $V(I)$ scaling exponent = 2. A $1 \mu\text{V/cm}$ criterion was used for J_c .

Transport critical current density (J_c) measurements at Air Force Research Laboratory (AFRL) were made in liquid nitrogen at 77.2 K with the 4-pt probe method (self-field) using pogo pins for current contacts [14], and a $1 \mu\text{V/cm}$ criterion. Systems to measure temperature and critical current were calibrated on a regular basis. Current was applied to the sample by a step-ramp method: a current step interval of 0.2 to 0.5 s, a ramp rate of 0.25 to 1.0 A/s, and a voltage sample period 2 to 4 times smaller than the current step interval. The maximum current step size was 0.2 A. Measurements of J_c were repeatable for these ranges of step-ramp parameters. Current sources and voltmeters for measurements were calibrated on a regular basis.

At AFRL, the superconducting transition temperature (T_c) was measured using an ac susceptibility technique with the amplitude of the magnetic sensing field, h , varied from 0.025 Oe to 2.2 Oe, at a frequency of approximately 4 kHz [15]. Note that the ac susceptibility technique provides information about primary and secondary transitions of the entire film, rather than a defined path that is obtained with transport T_c measurements. T_c s were measured immediately after film deposition and prior to adding Ag contacts. Samples were mounted onto the end of a sapphire rod and measured as the samples were warmed through the transition region at very slow rate of $\sim 0.06 \text{ K/min}$. The T_c measurements were accurate within $\leq 0.1 \text{ K}$ at three calibration points: liquid He at 4.2 K, liquid N_2 at 77.2 K, and room temperature.

Magnetic J_c measurements were made with a vibrating sample magnetometer (VSM) by Quantum Design using a ramp rate of $\sim 8000 \text{ A/m}\cdot\text{s}$ and a VSM at Ohio State University at ramp rates from 9,000 ($\text{A/m}\cdot\text{s}$) to 42,000 ($\text{A/m}\cdot\text{s}$). The J_c of the square samples was estimated using a simplified Bean model of $J_c = 15\Delta M/R$, where M is magnetization/volume from M-H loops, and R is the radius of volume interaction = square side for consistency [16]. The film thickness and dimensions of each sample were measured multiple times to reduce errors of superconducting volume and R to $< 5 \%$.

RESULTS and DISCUSSION

The surface microstructures resulting from multilayer deposition on RABiT's substrates are shown in Figure 1, compared to 123 films deposited on similar substrates. Particulate defect formation on the upper surface of composite films is greatly reduced and almost eliminated, compared to 123 films. Also in Figure 1 on viewing at high magnification, grains of the 123 phase about 0.3 micron size can clearly be seen in the 123 films, but are not present in the multilayer films. Both reduction of defect particulates and increased surface smoothness are consistent with previous results of multilayer films on single crystal LaAlO_3 or SrTiO_3 substrates, especially at greater thicknesses [10]. Both 123 and multilayer films had void defect formations, which were slightly enhanced for the multilayer films. However void formation can also be influenced by subtle properties of the buffer layers as observed in different 123/RABiT's films, therefore the difference of void formation observed in Figure 1 for multilayer and 123 films is not necessarily a consistent effect. The grain boundaries in both 123 and multilayer films showed enhanced formation of voids. The relative size and density of void formations at the grain boundaries could not be easily determined, because a large variation of void densities were observed at different grain boundaries even within a single sample.

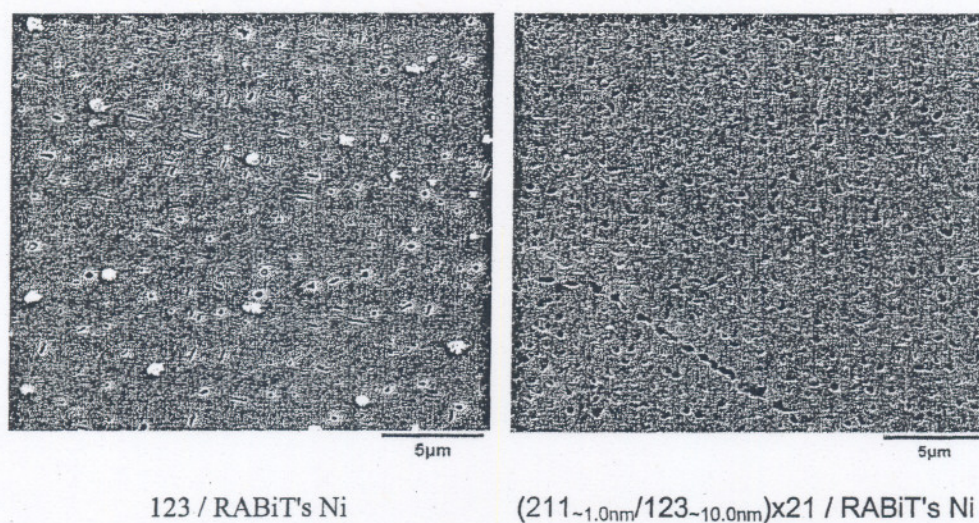


Figure 1. Scanning electron micrographs of surface microstructures of multilayer films (right) to 123 films (left), both on in-situ RABiT's substrates.

The critical current densities of the multilayer films are shown in Figure 2 along with 123 films deposited onto RABiT's substrates by the ex-situ BaF_2 process, as well as 123 films deposited on LaAlO_3 single crystal substrates. Compared to 123/RABiT's films, the critical current densities of multilayer films were slightly suppressed at $H_{\text{appl}} < 1.5$ T, however began increasing for fields > 1.5 T. Interestingly, the J_c improves at higher fields compared to 123 films deposited onto single crystal substrates, indicating that the pinning mechanism is significantly different in the multilayer films compared to 123 films. Self-field J_{cS} (77K, 0T) of $(0.7-1.0)$ MA/cm² were also measured for separate films deposited on in-situ RABiT's substrates, consistent with values in Figure 2 for ex-situ RABiT's substrates. The plots of normalized $J_c/J_c(0T)$ for the curves from Figure 2 are indicated in Figure 3. The increase of pinning in Figure 3 for multilayer films again

indicates the pinning mechanism is different, when compared to 123 films deposited onto single crystal or RABiT's substrates.

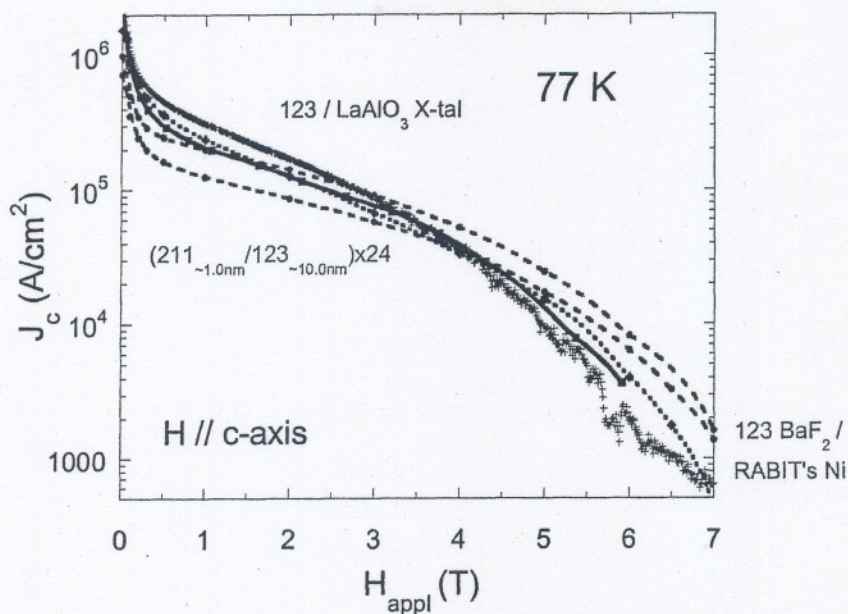


Figure 2. Critical current density at 77 K for $(211_{-1.3\text{nm}}/123_{-11.8\text{nm}})_{\times 26}$ multilayer films (\bullet) deposited onto ex-situ RABiT's substrates, 123 films on LaAlO_3 ($+$), 123 films on LaAlO_3 at 75 K (\blacksquare) [8], and the average value of 4 measurements of 123 films on $\text{CeO}_2/\text{YSZ}/\text{Y}_2\text{O}_3/\text{RABiT's NiW}$ ex-situ substrates (\blacklozenge).

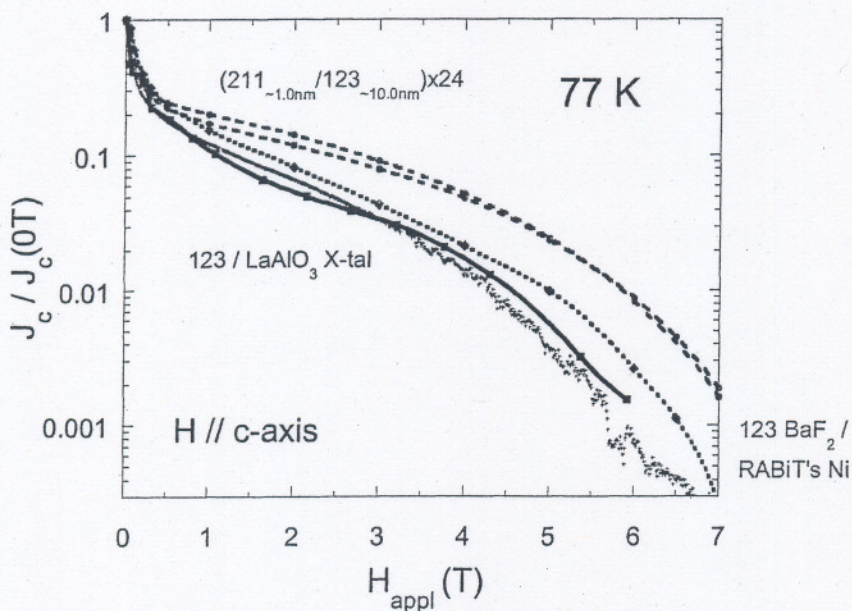


Figure 3. $J_c/J_c(0T)$ of films in Figure 2. H_{irr} for the multilayer films were (6.9-7.2) T.

Superconducting T_c s for multiple films deposited on in-situ and ex-situ RABiT's substrates were in the range of (88.5-89.5) K, as measured both at ORNL and AFRL. These T_c s were virtually identical to T_c s of multiple 123 films grown on both in-situ RABiT's substrates and single crystal LaAlO_3 substrates for exact same deposition conditions.

Finally, we note that a significant difference between the initial multilayer films deposited on RABiT's substrates compared to more optimized films deposited on single crystal substrates could well be that enhanced deposition of 211 nanoparticles occurs on the slightly misaligned ($0-8^\circ$) angle grain boundaries which are present in RABiT's substrates, however are not in single crystal substrates. For deposition of 211 nanoparticles on 123 surfaces, it was observed that 211 nanoparticles nucleate/form/coalesce preferentially on plateau or step edges and especially uneven points of plateaus or ledges, which presumably are energetically favorable sites. Therefore it's expected that on/near the RABiT's grain boundaries, even greater precipitation and coalescence of 211 nanoparticles might occur by this mechanism. Increasing the 211 particle density at the grain boundaries could enhance flux pinning there at greater applied fields, but may also reduce the critical current flow for zero-or-low applied magnetic fields if the density is too great at these sites. The J_c data supports this hypothesis, as an increase of J_c was observed for $H > 1.5$ T as shown in Figure 2 for RABiT's substrates which is a higher field than the value of $H > 0.1$ T on single crystal substrates when a J_c increase was observed [10]. However the J_c decrease in Figure 2 for $H < 1.5$ T might also have been caused by slight variations of deposition conditions or non-optimization of the process only for those depositions. Additional testing is necessary to determine which effect is occurring.

CONCLUSIONS

Transport J_{cs} (77K, self-field) = (0.6-1.0) MA/cm² were consistently achieved with AFRL and ORNL textured RABiT's substrates, as measured both at AFRL and ORNL. Transition temperatures $\sim 89-90$ K were measured at both AFRL and ORNL for all depositions; which were virtually the same as T_c s on LaAlO_3 single crystal substrates for these deposition conditions. Transport J_{cs} (77K, H_{appl}) were reduced slightly for $H_{\text{appl}} < 1.5$ T when compared to similar depositions on single crystal substrates, consistent with a hypothesis that enhanced deposition of 211 nanoparticles might have occurred at the misaligned angle of the grain boundaries which reduced the lower-field critical current flows. However a consistent increase of transport J_c was observed for $H_{\text{appl}} > 1.5$ T. The J_c (77K, H_{appl}) was higher than for J_c of 123 films on single crystal substrates for $H_{\text{appl}} > 4$ T. Normalized $J_c/J_c(0T)$ showed significantly different dependence on H_{appl} for multilayer films compared to 123 films, regardless of the substrate used. The improvement of normalized J_c suggests that if the $J_c(0T)$ of multilayer films can be improved with better processing conditions, the absolute values of $J_c(H_{\text{appl}})$ can be increased significantly for the RABiT's substrates. The surface microstructure of multilayer films on RABiT's substrates had flat surfaces and greatly reduced particulate formation, similar to multilayer deposition on single crystal substrates. However void formations were observed similar to deposition of 123 on RABiT's, which may have resulted from defects in the buffer layer structure. Additional studies will determine if the $J_c(H)$ properties can be improved, or are intrinsically limited.

Possible advantages of multilayer deposition for coated conductors might be improved mechanical strength under bending stress, and reduced crack formation because of nanoparticle inclusions.

ACKNOWLEDGEMENTS

The authors would like to thank Ken Marken and Oxford Instruments for supplying textured Ni substrates for this work.

REFERENCES

1. A. Bourdillon, N. X. Tan Bourdillon, *High Temperature Superconductors: Processing and Science* (Academic Press, San Diego CA, 1994).
2. D. Larbalestier, A. Gurevich, D. Matthew Feldmann, A. Polyanskii, *Nature* **414**, 368 (2001).
3. M. Murakami; D. T. Shaw and S. Jin; *Processing and Properties of High T_c Superconductors Volume 1, Bulk Materials*; edited by S. Jin, (World Scientific Publishing Co. Pte. Ltd., NJ, 1993).
4. D. C. Larbalestier and M. P. Maley, *MRS Bulletin* Aug. (1993) p. 50.
5. Y. Iijima, K. Onabe, N. Tugaki, N. Tanabe, N. Sadakara, O. Kohno and Y. Ikeno, *Appl. Phys. Lett.* **60**, 769 (1992).
6. X. D. Wu, S. R. Foltyn, P. N. Arendt, W. R. Blumenthal, I. H. Campbell, J. D. Cotton, J. Y. Coulter, W. L. Hults, M. P. Maley, H. F. Safar and J. L. Smith, *Appl. Phys. Lett.*, **67**, 2397 (1995).
7. A. Goyal, d. P. Norton, J. D. Budai, M. Paranthaman, E. D. Specht, D. M. Kroeger, D. K. Christen, Q. He, B. Saffian, F. A. List, D. F. Lee, P. M. Martin, Klabunde, E. Hartfield and V. K. Sikka, *Appl. Phys. Lett.*, **69**, 1795 (1996).
8. S. R. Foltyn, E. J. Peterson, J. Y. Coulter, P. N. Arendt, Q. X. Jia, P. C. Dowden, M. P. Maley, X. D. Wu, D. E. Peterson, *J. Mater. Res.* **12(11)**, 2941 (1997).
9. T. Aytug, M. Paranthaman, S. Sathyamurthy, B. W. Kang, D. B. Beach, E. D. Specht, D. F. Lee, R. Feenstra, A. Goyal, D. M. Kroeger, K. J. Leonard, P. M. Martin, and D. K. Christen, in *ORNL Superconducting Technology Program for Electric Power Systems, Annual Report for FY 2001*, p. 1-32 at <http://www.ornl.gov/HTSC/htsc.html>.
10. T. Haugan, P. N. Barnes, I. Maartense, E. J. Lee, M. Sumption, C. B. Cobb, *J. Mat. Res.* **18**, 2618 (2003).
11. T. Haugan, P. N. Barnes, L. Brunke, I. Maartense, J. Murphy, *Physica C* **397**, 47 (2003).
12. R. Feenstra, T. B. Lindemer, J. B. Budai, and M. D. Galloway, *J. Appl. Phys.* **69**, 6569 (1991).
13. J. W. Ekin, T. M. Larson, N. F. Bergren, A. J. Nelson, A. B. Swartzlander, L. L. Kazmerski, A. J. Panson and B. A. Blankenship, *Appl. Phys. Lett.* **52**, 1819 (1988).
14. L. F. Goodrich, A. N. Srivastava, T. C. Stauffer, A. Roshko and L. R. Vale, *IEEE Trans Appl. Supercond.* **4**, 61 (1994).
15. I. Maartense, A. K. Sarkar, and G. Kozlowski, *Physica C* **181**, 25 (1991).
16. J. R. Thompson, L. Krusin-Elbaum, Y. C. Kim, D. K. Christen, A. D. Marwick, R. Wheeler, C. Li, S. Patel, D. T. Shaw, P. Lisowski, and J. Ullmann, *IEEE Trans Appl. Supercond.* **5**, 1876 (1995).